Hiding under the Carpet: A New Strategy for Cloaking

Jensen Li and J. B. Pendry

Blackett Laboratory, Imperial College London, London SW7 2AZ, United Kingdom

(Received 10 June 2008; revised manuscript received 7 August 2008; published 10 November 2008)

A new type of cloak is discussed: one that gives all cloaked objects the appearance of a flat conducting sheet. It has the advantage that none of the parameters of the cloak is singular and can in fact be made isotropic. It makes broadband cloaking in the optical frequencies one step closer.

DOI: 10.1103/PhysRevLett.101.203901 PACS numbers: 42.79.−e, 02.40.−k, 41.20.−q

Transformation optics [1–5] can be used to design a cloak of invisibility. In essence the cloak makes its contents appear to be very small and hence invisible. However there are three distinct topological possibilities: the cloaked object can be crushed to a point, to a line, or to a sheet. In the process of crushing the object becomes infinitely conducting but this does not present a problem for the first case because scattering from even highly conducting small objects vanishes with the size of object. The same is true of a very thin object, i.e., a wire, because very thin wires have very large inductance and are therefore invisible to radiation. This is not true of the third possibility. Obviously a conducting sheet is highly visible unless of course it sits on another conducting sheet (the "carpet" of the title). Although this third possibility has limited cloaking potential it does have the considerable advantage that the parameters of the cloak need not be singular and, as we shall show, can be isotropic.

Several works investigated the cylindrical cloak with first experiment done in microwave [5–9]. Apart from transformation optics, there are other approaches in the subwavelength [10,11] and the geometrical optics regime [12] as well. Here, we use the first approach for its variety in applications [13,14]. Metamaterials are usually used to obtain the wide range of permittivity and permeability and there is a general quest to push the working wavelength to optical range. However, scaling down the magnetic resonating structures for the metamaterials causes severe absorption [15–19]. One solution is to use reduced material parameters and only metamaterials with electric resonating elements are needed for cloaking [20]. However, as long as resonating structures are used, materials absorption cannot be neglected.

In this work, instead of the complete cloak, we consider a cloak to mimic a flat ground plane. We will show that it does not require singular values for the material parameters; the range for the permittivity and the permeability is much smaller than in the case of a complete cloak. Moreover, by choosing a suitable coordinate transform, the anisotropy of the cloak can be minimized. As a result, only isotropic dielectrics are needed to construct the cloak. It greatly reduces absorption and makes broadband cloaking one step closer. For example, an object can now be compressed (or perceived) as a thin metal plate. The cloak works in a background dielectric (e.g., silica) so that it can be useful in designing optical integrated circuits.

For simplicity, we consider the 2D wave problem with E polarization. Fields are invariant in z direction. A ground plane here means a highly reflective metal surface. It is regarded as a perfect conductor. Suppose an object lies on it, a cloak is covered on the object so that the system is perceived as a flat ground plane again. The object is concealed between the cloak and the original ground plane as shown in Fig. 1(a). We assume the cloak (shown in cyan color) is a rectangle of size $w \times h$ except that the bottom (inner) boundary is curved upwards to leave enough space for the object. The whole configuration is called the physical system with coordinate (x, y) or (x^1, x^2) in indexed notation. The virtual system, shown in Fig. 1(b), is the configuration observer perceives. Its coordinate is labeled by (ξ, η) or (ξ^1, ξ^2). In general, we consider a coordinate transform which maps a rectangle $(0 \le \xi \le w, 0 \le \eta \le h)$ in the virtual system to an arbitrary region (the cloak) in the physical system.

We introduce the Jacobian matrix Λ by

$$\Lambda^i_{i'} = \frac{\partial x^i}{\partial \xi^{i'}}, \tag{1}$$

and the covariant metric g by

$$g_{i'j'} = \xi_{\mathbf{i}'} \cdot \xi_{\mathbf{j}'} \quad \text{or} \quad g = \mathbf{\Lambda}^{\mathbf{T}}\mathbf{\Lambda}, \tag{2}$$

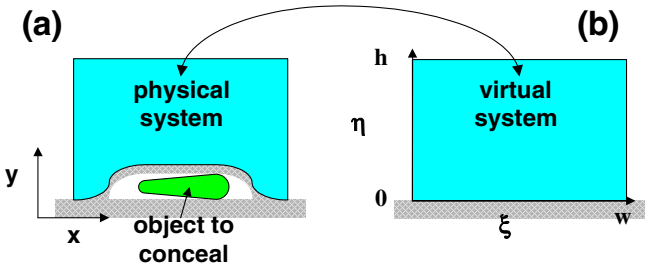

FIG. 1 (color online). The virtual and the physical systems. The regions in cyan are transformed into each other. Shaded regions represent the ground planes. The observer perceives the physical system as the virtual one with a flat ground plane.

where ξ_1, ξ_2 are the basis vectors of the virtual coordinates appearing in the physical system. For cloaking, the observer perceives the physical system as an isotropic homogeneous medium of permittivity ε_{ref} and unit permeability. The corresponding physical medium induced by the coordinate transformation is given by

$$\varepsilon = \varepsilon_{\text{ref}}/\sqrt{\det g}, \qquad [\mu^{ij}] = \Lambda\Lambda^T/\sqrt{\det g}. \tag{3}$$

We write μ_T and μ_L be the principal values of the permeability tensor in the physical medium and the corresponding refractive indices be $n_T = \sqrt{\mu_L \varepsilon}$ and $n_L = \sqrt{\mu_T \varepsilon}$ for the two (local) plane waves traveling along the two principal axes. To indicate the extent of anisotropy in the physical medium, the anisotropy factor α (a function of position) is defined by

$$\alpha = \max(n_T/n_L, n_L/n_T). \tag{4}$$

By using Eq. (2) and (3), it can be proved that

$$\alpha + \frac{1}{\alpha} = \frac{\text{Tr}(g)}{\sqrt{\det g}}, \tag{5}$$

with

$$\mu_L \mu_T = 1. \tag{6}$$

On the other hand, we define an averaged refractive index n relative to the reference medium by

$$n = \sqrt{n_L n_T}/\sqrt{\varepsilon_{\text{ref}}}, \tag{7}$$

so that

$$n^2 = \varepsilon/\varepsilon_{\text{ref}} = 1/\sqrt{\det g}. \tag{8}$$

Instead of using ε and μ^{ij} to describe the physical medium, we now use α and n (related to the ratio and the product of n_T and n_L) which have geometrical meanings in terms of the metric. If there is a very fine rectangular grid in the virtual domain with tiny cells of size $\delta \times \delta$, every such tiny square is transformed to a parallelogram in the physical domain with two sides $\xi_1\delta$ and $\xi_2\delta$. A smaller anisotropy means a smaller value of $\text{Tr}(g)/\sqrt{\det g}$ while a smaller area of the transformed cell ($\sqrt{\det g}\delta^2$) means a larger refractive index n.

In cloaking, compression of space in the physical domain essentially makes the cloak anisotropic. However, our heuristic approach is to minimize the induced anisotropy by choosing a suitable coordinate transform. If the anisotropy is small enough, we can simply drop it (by assigning $\alpha = 1$) and only keep the refractive index n. In other words, the physical medium becomes just a dielectric profile described by Eq. (8) with unit magnetic permeability.

In this work, such an optimal map is generated by minimizing the Modified-Liao functional [21]

$$\Phi = \frac{1}{hw}\int_0^w d\xi \int_0^h d\eta \frac{\text{Tr}(g)^2}{\det g}, \tag{9}$$

upon slipping boundary condition. Slipping boundary condition means that each of the four bounding edges of the virtual domain must be mapped to the four specified boundaries in the physical domain, only up to a sliding freedom. The minimal of this functional occurs at the quasiconformal map [22]. Without further technical proof, we state that the quasiconformal map actually minimizes not only the average but also the maximum value of $\text{Tr}(g)/\sqrt{\det g}$ in the physical domain, i.e., anisotropy minimized. Moreover, every little cell in the transformed grid in the physical domain is now a rectangle of constant aspect ratio M: m where M is called the conformal module of the physical domain (a geometrical property of the physical domain once the four boundaries are specified) and $m = w/h$ is the conformal module of the virtual domain, i.e.,

$$|\xi_1|/|\xi_2| = M/m, \qquad \sqrt{\det g} = |\xi_1||\xi_2|. \tag{10}$$

By substituting Eq. (10) into Eq. (5), we have

$$\frac{\text{Tr}(g)}{\sqrt{\det g}} = \frac{M}{m} + \frac{m}{M}, \quad \text{or} \quad \alpha = \max\left(\frac{M}{m}, \frac{m}{M}\right), \tag{11}$$

independent of position. We note that, the quasiconformal map approaches the conformal map [12] in the limit $M = m$. In general, a quasiconformal map is required for an unchanged topology of space without creating additional singular points in the coordinate transformation.

As a first example, let us map the area of a rectangle bounded by $0 \le \xi^1 \le 4$, $0 \le \xi^2 \le 1.5$ in the virtual domain to the same rectangle in the physical domain but with the bottom boundary specified by

$$y_{\text{bottom}}(x) = \begin{cases} 0.2\cos(\pi x/2)^2 & 1 \le x \le 3, \\ 0 & \text{otherwise.} \end{cases} \tag{12}$$

The transformed area in the physical domain becomes the cloak later. Figure 2(a) shows the transformed grid in the physical system if simple transfinite interpolation is used for a regular 40×15 grid. In this case, the grid is just a linear compression in the y direction. The anisotropy factor α, from Eq. (5), ranges from 1 to 1.385 while n^2, from Eq. (8), ranges from 1.0 to 1.153. On the other hand, for the generated grid using quasiconformal map, shown in Fig. 2(b), the grid lines are orthogonal. The aspect ratio of each cell or the anisotropy factor α becomes a constant of 1.042 while n^2 ranges from 0.68 to 1.96. The minimum (maximum) of n occurs on the inner cloak boundary at around $x = 1/x = 2$ where the cell area is largest (smallest). Therefore, we sacrifice n to a larger range while the anisotropy is minimized. Nevertheless, n or ε stays finite without approaching either zero or infinity. It is the result of crushing the object to a plane instead of a line. No singular points occur in the coordinate transform. We have also employed a smooth inner cloak boundary without additional corners (e.g., in the transformation used in Ref. [12]) to achieve a smaller range of n. The small

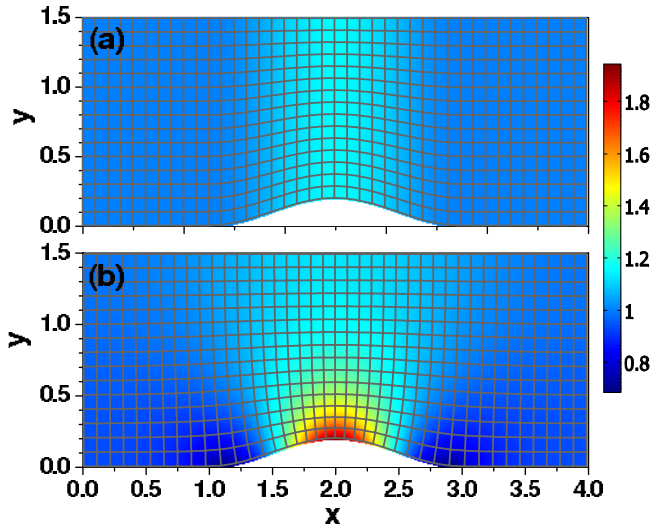

FIG. 2 (color online). The transformed grid in physical system with inner cloak boundary specified by Eq. (12) for (a) the transfinite grid and (b) the quasiconformal grid. The color maps show profile n^2.

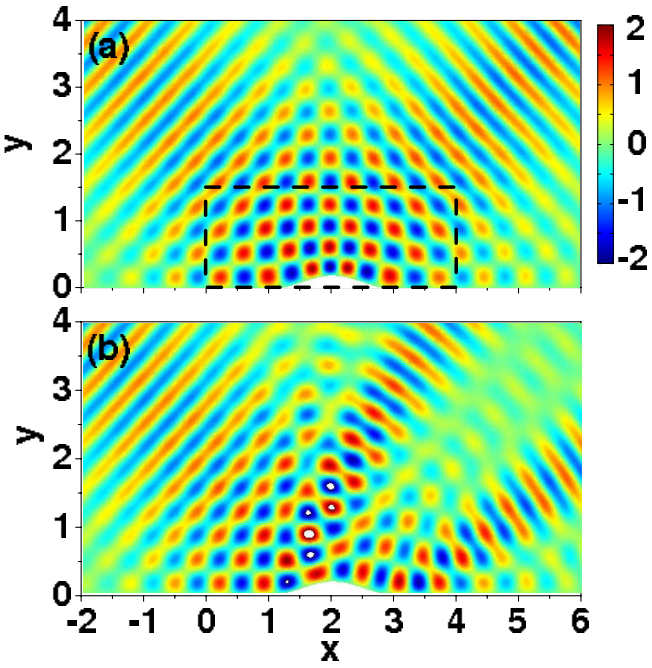

FIG. 3 (color online). (a) E-field pattern with the cloak located within the rectangle in dashed line when a Gaussian beam is launched at 45° towards the ground plane from the left. (b) E-field pattern when only the object (a reflecting surface of the shape of the inner cloak boundary) is present without the cloak. All lengths are in μm. The width of the beam is 4 μm at a wavelength of 750 nm. The background is SiO_2.

anisotropy together with the finite range of n makes realization of the cloak easier.

To test the effectiveness of the designed cloak, suppose the cloak is 4 μm by 1.5 μm; i.e., the length unit in the previous discussion is in μm and the cloak is defined relative to silica (SiO_2) of $\varepsilon_{\text{ref}} = 2.25$. We employ the quasiconformal grid but ignore the anisotropy in the cloak by only keeping the ε profile with unit permeability. In this case, the permittivity of the cloak varies from around 1.5 to 4.4. This range can be obtained effectively by etching or drilling subwavelength holes of different sizes along the z direction in a high dielectric, e.g., Si. Outside the cloak, it is again the silica as background material. Moreover, the inner surface of the cloak is coated by a highly reflective metal. To the observer, it is perceived as if this is the actual ground plane. This is relevant to the situation of routing light at our own will in optical integrated circuits. Suppose a Gaussian beam at a wavelength of 750 nm (i.e., 500 nm in SiO_2) is launched at an angle of 45° to the object together with the cloak, the total E-field pattern (real part) obtained from a finite-element simulation is shown in Fig. 3(a). The cloak is within the rectangle in dashed line in the figure. The field outside the cloak resembles the field as if we only have a flat ground plane. A reflected beam at 45° is clearly seen. There are no spurious reflections from the three boundaries between the cloak and the background material since the permittivity at the cloak boundary returns effectively to the background material. This can be revealed from the quality of the grid shown in Fig. 2(b) as the cells at the three boundaries are nearly squares of the same size. Moreover, the field inside the cloak shows interference pattern between the incident and the reflected beam. The pattern is simply squeezed upwards, comparing to the field when only a flat ground plane is present. The E-field pattern with only the object present is also shown in Fig. 3(b) for comparison. The incident beam is deflected and split into two different angles at around 38° and 53° by examining the field farther away. Therefore, the cloak successfully mimics a flat ground plane.

We emphasize that our strategy is valid in both geometrical and wave optics. In fact, the demonstrated cloak is broadband in nature since the frequency dispersion (and also the losses) of the dielectrics can be made very small. For example, a Gaussian wave packet centered at a wavelength of 750 nm is launched to the object and the cloak at 45°. The transverse width of the packet is 2 μm with a duration of 20 fs (8 periods of central frequency). It results an incident packet with circular spatial profile at time $t = 0$, as shown in Fig. 4(a). After a duration of 14.8 periods at $t = 37$ fs, the packet is reflected back at 45° with the same Gaussian shape of nearly no distortions, as shown in Fig. 4(b). If the cloak is absent, the wave packet is split into two elongated packets, as shown in Fig. 4(c). It is thus a time-domain cloaking effect. However, if a thinner cloak or bigger object is used, the distortion will become larger due to a larger anisotropy neglected in the cloak profile.

We have only considered a perfect conductor as the bottom boundary but results look very similar if realistic silver with absorption is used. Moreover, the cloak also

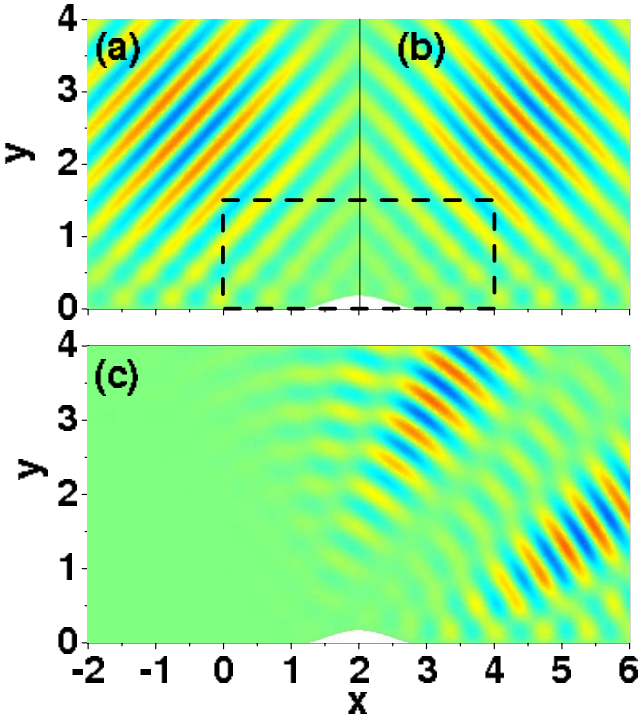

FIG. 4 (color online). (a) E-field pattern of the incident wave packet at time $t = 0$. A Gaussian wave packet with 2 μm in spatial width and 20 fs in time width (at a central wavelength of 750 nm) is launched at 45° towards the ground plane from the left. (b) E-field pattern showing the reflected packet from the cloak at time $t = 37$ fs. (c) E-field pattern at time $t = 37$ fs when the cloak is absent. All length scales are in μm. The background is SiO_2.

works for the H polarization. For example, when the cloak is mirrored in the y direction, it becomes a directional cloak so that the object can be compressed to be a thin metal plate, becoming invisible for a plane wave traveling in x direction. In this work, instead of cloaking an airplane in the sky, our cloak is more relevant to cloaking a tank on the ground. Recently, there is a work on cloaking over a dielectric half-space using a singular cloak [23]. However, extending our nonsingular mapping scheme to a more general boundary, like a dielectric, is outside the scope of this work.

In conclusion, a cloak is designed to mimic a flat ground plane. The coordinate transform induces no extreme values in the material profile. Moreover, the quasiconformal map is the optimal one to minimize the anisotropy of the cloak. The small anisotropy is further neglected so that the cloak can be constructed by only isotropic dielectrics. It relieves the loss issue by avoiding the usage of resonating elements and is a step closer to do broadband transformation optics at optical frequencies. The quasiconformal map should also be a convenient technique for both polarizations as well and in other applications in transformation optics.

J. L. would like to acknowledge support from the Croucher Foundation from Hong Kong. J. B. P. thanks the EPSRC for financial support.

[1] A. J. Ward and J. B. Pendry, J. Mod. Opt. **43**, 773 (1996).
[2] D. Schurig, J. B. Pendry, and D. R. Smith, Opt. Express **14**, 9794 (2006).
[3] U. Leonhardt and T. G. Philbin, New J. Phys. **8**, 247 (2006).
[4] J. B. Pendry, D. Schurig, and D. R. Smith, Science **312**, 1780 (2006).
[5] D. Schurig *et al.*, Science **314**, 977 (2006).
[6] S. A. Cummer *et al.*, Phys. Rev. E **74**, 036621 (2006).
[7] F. Zolla, S. Guenneau, A. Nicolet, and J. B. Pendry, Opt. Lett. **32**, 1069 (2007).
[8] Z. Ruan *et al.*, Phys. Rev. Lett. **99**, 113903 (2007).
[9] B. Zhang *et al.*, Phys. Rev. B **76**, 121101(R) (2007).
[10] A. Alu and N. Engheta, Phys. Rev. E **72**, 016623 (2005).
[11] G. W. Milton and N.-A. P. Nicorovici, Proc. R. Soc. A **462**, 3027 (2006).
[12] U. Leonhardt, Science **312**, 1777 (2006).
[13] M. Rahm *et al.*, Photon. Nanostr. Fundam. Appl. **6**, 87 (2008).
[14] H. Chen and C. T. Chan, Appl. Phys. Lett. **90**, 241105 (2007).
[15] Stefan Linden *et al.*, Science **306**, 1351 (2004).
[16] V. M. Shalaev *et al.*, Opt. Lett. **30**, 3356 (2005).
[17] S. Zhang *et al.*, Opt. Express **13**, 4922 (2005).
[18] G. Dolling *et al.*, Opt. Lett. **31**, 1800 (2006).
[19] G. Dolling *et al.*, Opt. Lett. **32**, 53 (2007).
[20] W. Cai *et al.*, Nat. Photon. **1**, 224 (2007).
[21] P. Knupp and S. Steinberg, *Fundamentals of Grid Generation* (CRC Press, Boca Raton, 1994).
[22] J. F. Thompson, B. K. Soni, and N. P. Weatherill, *Handbook of Grid Generation* (CRC Press, Boca Raton, 1999).
[23] P. Zhang, Y. Jin, and S. He, Opt. Express **16**, 3161 (2008).